Lead isotope systematics of porphyry–epithermal spectrum of the Birgilda–Tomino ore cluster in the South Urals, Russia

Olga Plotinskaya, ndrey V. Chugaev, Reimar Seltmann

PII: S0169-1368(16)30535-2
DOI: doi: 10.1016/j.oregeorev.2016.09.006
Reference: OREGEO 1930

To appear in: *Ore Geology Reviews*

Received date: 4 July 2016
Revised date: 29 August 2016
Accepted date: 5 September 2016

Please cite this article as: Plotinskaya, Olga, Chugaev, ndrey V., Seltmann, Reimar, Lead isotope systematics of porphyry–epithermal spectrum of the Birgilda–Tomino ore cluster in the South Urals, Russia, *Ore Geology Reviews* (2016), doi: 10.1016/j.oregeorev.2016.09.006

Lead isotope systematics of porphyry–epithermal spectrum of the Birgilda–Tomino ore cluster in the South Urals, Russia

Olga Yu. Plotinskaya[a,*], Andrey V. Chugaev[a], Reimar Seltmann[b]

[a]Institute of Geology of Ore Deposits, Petrography, Mineralogy, and Geochemistry Russian Academy of Sciences (IGEM RAS), Staromonetny per. 35, Moscow 119017,Russia
[d] Centre for Russian and Central EurAsian Mineral Studies (CERCAMS), Department of Earth Sciences, Natural History Museum, London SW7 5BD, United Kingdom

*Corresponding author. E-mail address: plotin@igem.ru

Abstract

The paper provides the first data on lead isotopic composition of porphyry and epithermal mineralization of the Birgilda-Tomino ore cluster. Lead isotope characteristics were obtained for 24 sulfide samples representing epithermal Au-Ag (Bereznyakovskoe ore field and Michurino occurrence), base-metal carbonate replacement (Biksizak occurrence), porphyry copper (Tomino, Kalinovskoe, and Birgilda deposits), and four plagioclase samples of the Birgilda-Tomino Igneous Complex. Ore samples have lead isotopic signatures similar to neighboring intrusions of the Birgilda-Tomino igneous complex and this confirms genetic relations between epithermal Au-Ag, base-metal carbonate replacement and porphyry copper mineralization with diorite porphyry intrusions. Variations in lead isotopic composition are caused by mixing of mantle and crustal lead sources. The input of radiogenic ^{206}Pb took place during the post-ore phase as a result of a series of tectono-magmatic events, which include emplacement of at least two phases of the Chelyabinsk pluton. The latter however could act only as a trigger of hydrothermal activity but not as a lead source.

Keywords: Porphyry; epithermal; lead isotopes; Urals

1. Introduction

Porphyry copper deposits are known to be formed in various geodynamic settings (Sillitoe, 2010) and thus various sources of magma, fluid, and metals can be involved in the system. Distinct crustal/mantle ratios may reflect ore geochemistry and even the economic potential and thus are of a great interest. Pb-Pb isotopic systematics is a clue to distinguish between mantle and crustal components in parental magma and fluid, especially when combined with Sm-Nd and Rb-Sr data. Unfortunately, for the Urals this approach remained hitherto neglected. Few Pb and Sm-Nd isotopic studies concern only VHMS deposits (Vinogradov et al., 1960; Spadea and d'Antonio, 2006; Chernyshev et al., 2008; Tessalina et al., 2016 and references therein). However Sm-Nd and Rb-Sr isotope systematics were studied for most porphyry deposits of the Urals (Grabezhev, 2009).

In this paper we provide first data on lead isotopic compositions of porphyry and epithermal mineralization in the Birgilda-Tomino ore cluster. The latter, located ca. 30 km south from the city of Chelyabinsk, is one of the key sites in the Urals where porphyry and epithermal mineralization styles of Paleozoic age were preserved (Plotinskaya et al., 2014 and references therein).

2. General geology

2.1. Tectonic setting

The Birgilda-Tomino cluster is located within the East-Uralian Volcanic terrane which is interpreted to be overthrusted onto the East-Uralian Sialic megaterrane (Fig. 1, inset). The latter is composed of gneiss and granite-gneiss complexes of Paleo- to Early-Mesoproterozoic age and in the Neoproterozoic (in Russian literature traditionally referred to as Late Riphean to Vendian) this terrane represented the East-Uralian microcontinent surrounded by the Paleo-Uralian ocean (Samygin and Burtman, 2009 and references therein). In the Neoproterozoic this microcontinent was covered by terrigenous quartz and polymictic sediments.

The East-Uralian Volcanic terrane, which comprises fragments of Paleozoic volcanic arc terranes, is interpreted as a part of the Silurian intra-oceanic volcanic arc that formed due to westward (Samygin and Burtman, 2009; Puchkov, 2016 and references therein) or eastward (Yazeva and Bochkarev, 1995) subduction (here and throughout the text we mean the present-day coordinates). This arc was named as the Eastern (Vostochnaya) arc (Yazeva and Bochkarev, 1998) or Transuralian arc (Puchkov, 2016). This arc could have been the southern end of the Tagil arc or one developed independently (Yazeva and Bochkarev, 1995; Puchkov, 2016). Both statements are still open to debate (Snachev et al., 2006; Tevelev et al., 2006). Volcanic activity ceased in the Early Devonian (Lochkovian) and subduction "jumped" westward to form the Magnitogorsk arc (Yazeva and Bochkarev, 1995). By that time the "Eastern arc" was supposedly accreted to the East-Uralian microcontinent (Yazeva and Bochkarev, 1995).

New westward directed subduction process under the East-Uralian microcontinent began in the Late Devonian to Early Carboniferous and resulted in formation of the Andean-type arc with emplacement of intrusions of gabbro-tonalite-granodiorite-granite series (Bea et al., 2002; Fershtater, 2013). The closure of the Paleo-Uralian ocean and collision between the East European plate and the Kazakh continent in the Late Carboniferous (Moscovian) led to the formation of the Uralian orogen (Samygin and Burtman, 2009) and emplacement of sub-alkaline granite series of Permian age (Bea et al., 2002; Fershtater, 2013).

2.2. General geology of the Birgilda-Tomino cluster

It should be noted that the described territory, like most of south to southeast Urals peneplain, has a

relatively flat topography with weathering crust extending to depths of 20 – 40 m. This compromises geological observations and most geological information was derived from drilling.

Neoproterozoic (Riphean) rocks are exposed outside of the described area and have tectonic contacts with younger formations (Puzhakov et al., 2013). The northeastern part of the territory (Fig. 1) comprises the Early to Middle Ordovician **Sargazy** Formation with a maximum thickness of 1500 m. It is composed of aphyric basalt and andesitic basalt supplemented by minor porphyric basalt and basaltic volcanoclastic rocks, as well as rhyolite and rhyolite tuffs metamorphosed in greenschist facies (actinolite-epidote-chlorite, epidote-chlorite, epidote-carbonate-chlorite, and epidote-sericite subfacies) (Puzhakov, 1999). They were reported to belong to the Na-calc-alkaline bimodal series (Puzhakov, 1999; Puzhakov et al., 2013). The Sargazy Formation was attributed to the Ordovician based on geological observations (Puzhakov et al., 2013) whereas Yazeva and Bochkarev (1995) suppose it represents Llandoverian volcanic arc basalts typical for young oceanic arcs.

The **Voznesensky** gabbro–diorite–plagiogranite pluton located in the northwest was interpreted to be co-magmatic with the Sargazy Formation (Grabezhev et al., 1998) but recent U-Pb dating of zircons from diorite yelded ages of 328 ± 4 and 326 ± 3.5 Ma (Puzhakov et al., 2013) and led to the conclusion that at least some phases are related to another magmatic event. In the central part of the area, the Sargazy basalts are overlain with angular unconformity by sedimentary rocks of the Middle Ordovician to Lower Silurian limestones and marbles of the **Biksizak** Formation, up to 130 m thick.

Two aforementioned formations are overlain with angular unconformity by volcanics of the **Bereznyakovskoe** Formation. These are up to 1000 m thick andesitic dacite volcanoclastic rocks and minor lava with rare limestone interlayers (Grabezhev et al., 1998; Puzhakov, 1999). Numerous diorite and andesite porphyry stocks of the **Birgilda–Tomino Igneous Complex** which is thought to be comagmatic with the Bereznyakovskoe Formation are known throughout the area (Grabezhev et al., 1998; Puzhakov, 1999).

Age of the Bereznyakovskoe Formation and the Birgilda–Tomino Igneous Complex has been debated for tens of years. The main reason is that the Bereznyakovskoe Formation has tectonic contacts with most sedimentary rocks known in the area which itself was only poorly studied. Initially both the Bereznyakovskoe Formation and the Birgilda–Tomino Igneous Complex were considered as Wenlock-Ludlow in age (Yazeva and Bochkarev, 1995 and references therein). Later their age was reassessed as the Late Devonian to Early Carboniferous based on K-Ar dating of sericite from the Bereznyakovskoe Au-Ag-epithermal and Tomino porphyry copper deposits (Grabezhev et al., 1998). This links both the Bereznyakovskoe Formation and the Birgilda–Tomino igneous complex with the age of the Late-Devonian to Early Carboniferous Andean-type volcanic arc formed above the subduction zone interpreted to have dipped westward under the East Uralian continent (Samygin and Burtman, 2009; Puchkov, 2013). Recent U-Pb SHRIMP dating of diorite from the Tomino and Bereznyakovskoe deposits

(Grabezhev et al., 2013) yielded zircon ages of 428 ± 3 Ma and 427 ± 6 Ma, while Re-Os dating of molybdenite from the Kalinovskoe deposit (Tessalina and Plotinskaya, this volume) revealed an age of 430.4 ± 2.0 Ma. This leads to the conclusion that they are related to the activity of the Silurian intra-oceanic arc (see section 2.1 above).

Upper Silurian to Middle Devonian limestone formations in excess of 1000 m thickness are known in the easternmost part of the territory. Limestones are overthrusted onto the Bereznyakovskoe Formation via a series of thrusts and nappes (Puzhakov, 1999). Givetian to Famennian sediments of the **Yemanzhelinsk** Formation (siltstones, schists, sandstones with minor limestone) up to 1000 m thick (Puzhakov et al., 2013), overlay limestone sequences with an angular unconformity. Visean andesite, andesitic basalt, andesitic dacite and their volcanoclastic varieties as well as trachyandesite of the **Tayandy** Formation overlie sediments with angular unconformity. Those are followed by Visean to Moscovian terrigenous-carbonate sequences (Puzhakov, 1999).

The **Chelyabinsk Pluton** located in the northernmost part of the area comprises two intrusive phases (Fershtater, 2013). The first one, related to the Late Devonian to Early Carboniferous subduction (Bea et al., 2002; Fershtater, 2013) comprises large (tens km across) bodies of a high-K calc-alkaline quartz diorite and granodiorite dated as 358 ± 5 Ma and 361 ± 5 Ma (U-Pb SHRIMP dating of zircon) respectively followed by 344 ± 5 Ma moderate-K biotite granite porphyry and 317 ± 12 Ma gneissic granite (Kallistov, 2014). The second phase is related to the Late Carboniferous to Permian collision and comprises the sub-alkaline granite, leucogranite porphyry and leucogranite dated by U-Pb SHRIMP method in zircon as 275 ± 3 Ma, 271 ± 5 Ma, and 260 ± 3 Ma respectively (Kallistov, 2014). Those form relatively small stocks up to 3-5 km in diameter (located outside of the Fig. 1). Small intrusions of garnet-muscovite leucogranite were interpreted to be of Triassic age (Ar-Ar method) and therefore post-orogenic (Osipova et al., 2010; Kallistov, 2014). Numerous small dikes of rhyolitic dacite, diabase, lamprophyre, and other rocks are known throughout the described territory. Most of them are thought to be linked to the Chelyabinsk Pluton.

2.3. Deposits and occurrences

Most deposits and occurrences are both spatially and genetically linked to diorite and andesite intrusions of the Birgilda-Tomino Igneous Complex (Grabezhev et al., 1998, 2000; Plotinskaya et al., 2014). The Ordovician basalts of the Sargazy Formation host Birgulda, Tomino, and Kalinovskoe copper porphyry deposits, the Middle Ordovician to Lower Silurian limestones of the Biksizak formation host the Biksizak base-metal occurrence while andesitic dacite tuffs of the Bereznyakovskoe Formation host epithermal Au-Ag deposits and occurrences.

2.3.1. Bereznyakovskoe Au-Ag epithermal ore field

The Bereznyakovskoe ore field is located in the southern part of the ore cluster (Fig. 1) and is hosted by andesite–dacite tuffs and lavas of the Bereznyakovskoe Formation, and by stocks of the Birgilda–Tomino Igneous Complex. The latter is represented mainly by subvolcanic andesites, which at depth give way to quartz diorite porphyry (Lehmann et al., 1999; Puzhakov, 1999).

The orefield comprises several sites, but the three major deposits (Bereznyakovskoe, South (Yuzhnoe), and Deputatskoe) host a total resource of approximately 36 t of gold (Fedoseev, 2007). Hypogene ore of high- to intermediate sulfidation style is accompanied by silica alteration with minor pyrophyllite, surrounded by haloes of sericite–quartz and quartz–sericite alteration. Three mineralization stages were proposed by Plotinskaya et al. (2009, 2014) for the Bereznyakovskoe ore field: (1) pyrite or early ore stage; (1) base-metal or main ore stage with enargite, fahlore–telluride, and Au-telluride assemblages; and (3) galena-sphalerite stage.

2.3.2. The Michurino Ag-Au-Cu-Pb-Zn occurrence

The Michurino Au-Ag–base-metal occurrence is hosted by tuffs, tuff breccias, and andesitic dacite lava of the Bereznyakovskoe Formation, intruded by subvolcanic andesites. The host rocks were affected by sericitic, chloritic and argillic alteration. Mineralization occurs as a stockwork of quartz-carbonate-sulfide veinlets and disseminated mineralisation, interpreted as sub-epithermal origin (Plotinskaya et al., 2014). Three stages were suggested: (1) quartz–pyrite (with rare chalcopyrite and bornite); (2) dolomite-base-metal (chalcopyrite, fahlore, galena, sphalerite, occasionally gold and Ag-Au and Bi tellurides); and (3) calcite-quartz (Plotinskaya et al., 2014).

2.3.3.The Biksizak base-metal occurrence

The Biksizak occurrence is located in the central part of the ore cluster. Mineralization, located at depths of approximately 250 to 350 m, is confined to the Late Ordovician to Early Silurian limestones of the Biksizak Formation, altered to ankerite-dolomite±silica rock (Grabezhev et al., 1998; Plotinskaya et al., 2010, 2015; Seravkin and Snachev, 2012). Mineralized interlayers of massive or disseminated sulfides are up to several meters thick and are separated by barren intervals up to 10 m thick. The ore manto is several hundred meters in plain view, gently dipping westward (Grabezhev et al., 1998). Pyrite and sphalerite are main ore minerals; fahlore, chalcopyrite, magnetite, hematite, galena and arsenopyrite are common; native gold, Ag sulfosalts, Au-Ag, Pb, Bi tellurides, and Co-Ni minerals are rare (Plotinskaya et al., 2010, 2014, 2015). A diorite intrusion in the westernmost part of the occurrence hosts uneconomic porphyry-style mineralization (Puzhakov, 1999). Six mineral assemblages were identified (Plotinskaya et al., 2015): (1) hematite–magnetite, (2) pyrite–arsenopyrite, (3) chalcopyrite–sphalerite, (4) fahlore–chalcopyrite, (5) gold–telluride, and (6) Ag–sulfosalt. This occurrence was classified as a

carbonate replacement base-metal mineralization related to a porphyry system (Plotinskaya et al., 2010).

2.3.4.The Tomino porphyry copper ore field

The Tomino ore field includes two relatively large stocks, each approx. 2 km in diameter, hosting the **Tomino** and **Kalinovskoe** sites as well as several smaller intrusions and occurrences, with total reserves of 331 Mt at 0.46% Cu and 0.1 g/t Au (Volchkov et al., 2015). Intrusions of the Birgilda-Tomino igneous complex are composed of quartz diorite, amphibole plagioclase diorite and their porphyry varieties, see also the detailed map in Tessalina and Plotinskaya (this volume). The porphyry mineralization occurs both in diorites and in hosting Ordovician basalts. In central zones of diorite stocks, **phyllic** alteration accompanies **chalcopyrite±bornite±molybdenite** mineralization, while in peripheral zone dominates **propylitic** alteration with **pyrite-chalcopyrite** mineralization and occasional magnetite and hematite. The latest stage mineralization, which occurs in the periphery of Kalinovskoe site, includes various Bi-sulfosalts, native gold, galena, sphalerite, tetrahedrite (Plotinskaya et al., 2014) and bornite to chalcopyrite with rare tellurides of Au-Ag, Ag, Pb, Bi, Hg. The oxidation zone, up to 40 m thick, contains malachite, azurite and chalcocite.

2.3.5. The Birgilda Cu-porphyry deposit

This was the first porphyry-style mineralization discovered in the territory of the ore cluster (Romashova, 1984). Mineralization is confined to two stocks of diorite and diorite porphyry approx. 1 km in size, namely South and North Birgilda sites, and occurs both in stocks and country rocks. Diorites are pervasively quartz-sericite (phyllic) and mixed chlorite-sericite altered, while propylitic (chlorite±epidote) alteration dominates in hosting basalts. Pyrite, chalcopyrite and molybdenite are the main ore minerals. Both mineralization and alteration are similar to those of the Tomino orefield. Romashova (1984), however, proposed a remarkable redistribution of ore assemblages due to the emplacement of the Chelyabinsk Pluton. Narrow zone of argillic alteration occurs in the Southern site. It accompanies quartz veinlets with base-metal mineralization (pyrite, chalcopyrite, galena, sphalerite, Pb-, Bi- and Ag-tellurides) in relation to intermediate argillic. Numerous quartz-calcite-pyrite veinlets represent the latest mineralization stage.

2.3.6. Other mineralization types

In addition to the afore-mentioned porphyry and porphyry-related mineralization, Grabezhev et al. (1998) reported the **Yaguzak** prospect with uneconomic porphyry Cu–Mo–Au mineralization, located in the western part of the territory. They suggested that this mineralization might be related to Carboniferous monzogranodiorite porphyries, with petrochemical features close to those of the

Chelyabinsk Pluton.

In the northeastern part of the territory several small **gold–quartz lode** deposits are known (Grabezhev et al., 1998; Snachev and Kuznetsov, 2011). They were classified as mesothermal or orogenic style, spatially associated with Carboniferous granodiorite porphyry dykes of the Chelyabinsk Complex. All of them had been mined since the middle of 19th century until the World War II and are not considered in this study.

3. Sampling

Samples, representing sulfide mineralization, were selected from different zones of the deposits and, where possible, from different assemblages or mineralization stages (Table 1 and Fig. 2). All samples were investigated by optical microscopy and most of them also by SEM-EDS in order to reveal mineral inclusions which might reflect lead isotope systematics. Because lead isotopic composition is controlled first of all by the presence of Pb-bearing minerals we paid special attention to those. E.g., in the Bereznyakovskoe ore field micron-scale inclusions of galena-clausthalite in enargite (Fig. 2a) control lead isotopic composition of the enargite assemblage and micron-scale inclusions of altaite in tennantite (Fig. 2b) do this for the fahlore-telluride assemblage. In the Michurino and Biksizak occurrences lead isotopic composition of ores is determined by small inclusions of galena (Fig. 2d,e), in samples from central zones of the Tomino and Kalinovskoe deposits representing early phyllic-related chalcopyrite-bearing assemblages (sample T-3501/120.5, Fig. 2f) no Pb-bearing phases were observed and these samples are believed to have their own unique lead isotopic systematics, which was not affected by later stages of hydrothermal activity. On the contrary, in samples from peripheral zones of the Kalinovskoe deposit micron-scale inclusions of galena-clausthalite in bornite were observed. They are confined to cracks or grain boundaries (Fig. 2i) and might be related to another hydrothermal event. It should be noted that most chalcopyrite and pyrite samples representing porphyry-style mineralization reveal lead concentrations below 5 ppm and were not suitable for precise isotopic analysis. These are not considered in this study.

Samples, representing magmatic rocks of the Birgilda-Tomino complex, were selected from places, where possible, distant from ore, and represent least altered rocks (Fig. 3a-d). In order to estimate possible influence of later magmatic events, we analyzed samples representing the largest phases of the Chelyabinsk Pluton (Fig. 3e-g) which were provided by T.A. Osipova (Zavaritsky Institute of Geology and Geochemistry, Yekaterinburg, Russia).

4. Analytical methods

4.1. XRF and ICP-MS analyses

Whole-rock major and trace element data were obtained at the Institute of Geology of Ore Deposits,

Petrography, Mineralogy and Geochemistry of the Russian Academy of Sciences (Moscow, Russia).

Major oxides and a number of minor elements (Cr, V, Co, Ni, Cu, Zn, Rb, Sr, Zr, Ba, As) in bulk rock samples were determined with AxiosmAX from PANalytical X-ray sequential fluorescence spectrometer. Samples were prepared by the fusion of 0.3 g powder with 3 g Li tetraborate in induction-arc furnace. The accuracy was 1–3% for the elements with concentrations above 0.5 wt % and up to 12% for those below 0.5 wt %. Loss on ignition (LOI) values were determined gravimetrically.

Trace elements (Y, Nb, Mo, Ag, Cd, Sn, Cs, La, Ce, Pr, Nd, Sm, Eu, Gd, Tb, Dy, Ho, Er, Tm, Yb, Lu, Hf, Ta, W, Pb, Bi, Th, U) were determined by the ICP-MS method using the XSeriesII instrument. Powdered samples (50–100mg) were digested in high-pressure Teflon Savillex vials, using a hot HF–HNO_3 mixture (5:1), followed by HCl in the Milestone microwave oven to ensure complete dissolution. Accuracy of the analyses was monitored by analyzing the USGS standards BHVO-1, AGV-1, and in-house reference materials with a periodicity of 10%. Accuracy for most trace elements was less than 1 to 3%, with the exception of Pb (up to 15%).

4.2. Lead isotope analyses

Lead isotopic analyses were performed at IGEM RAS (Moscow), using a NEPTUNE (ThermoFinnigan, Germany) mass spectrometer in a “wet” plasma regime. Sulfides were separated from the ore specimen under a microscope using needle or micro drill; feldspars were separated from the crushed whole rock using the standard procedure in the Mineral Separation Lab (IGEM RAS) from fractions 0.25 to 0.5mm (approx. 30 to 60 mesh) and after that handpicked under a stereomicroscope.

A detailed description of further sample processing and analytical procedure is given in Chernyshev et al. (2007). The galena samples below 0.001g were dissolved in 10M HNO_3 to prepare a solution with 3% HNO_3 with Pb concentration as much as 200 to 400 ng/ml. Sulfide and feldspar samples 0.04 to 0.07g were dissolved in Aqua Regia and HNO_3+HF mixture respectively. Lead was separated with an ion exchange chromatography; the details are described in Chugaev et al. (2013). Total blank did not exceed 0.15 ng. A Tl spike was added to the solutions before measurements; during measurements the current results were corrected for a mass-discrimination effect based on $^{205}Tl/^{203}Tl = 2.3889 \pm 1$. Reproducibility on the SRM 981, AGV-1 and BCR-1 standard samples during the course of the measurement (2σ) was ±0.02% for galena and ±0.03% for feldspar and sulfides. The U, Th and Pb concentrations in feldspar and sulfide (except of galena- and altaite-bearing) samples were measured by ICP–MS (IGEM RAS) in the same solutions. Lead isotopic ratios of feldspars and sulfides were corrected for radioactive decay using U, Th and Pb contents.

5. Results

5.1. Chemical composition of Birgilda-Tomino Igneous Complex

Chemical composition of rocks of the Birgilda-Tomino Complex selected for Pb isotope studies is presented in Table 2. All samples demonstrate high LOI due to weak to moderate sericite and carbonate alteration. Despite this, the rocks show similar chemical composition corresponding to diorites of the calc-alkaline series with Na_2O/K_2O from 0.13 to 0.28, similar to the published data (Grabezhev et al., 1998; Puzhakov, 1999; Plotinskaya et al., 2014; Plotinskaya et al., 2016).

The spider diagram (Fig. 4a) shows negative anomalies for all rocks in Nb and Ti and positive anomalies in Pb and Li, as well as a general enrichment in incompatible elements, a characteristic feature of arc magmas (Sun and McDonough, 1989; Pearce and Peate, 1995). The REE patterns show moderate LREE to HREE and LREE to MREE enrichment (La_n/Yb_n = 3.46 to 11.92, La_n/Sm_n=1.83 to 3.81) and no MREE to HREE enrichment (Dy_n/Yb_n=0.74 to 1.06). The weak Eu anomaly, negative for sample from the Bereznyakovskoe deposit and positive for one from the Kalinovskoe deposit, is likely to be result of hydrothermal overprint. The sample representing the post-ore diorite-porphyry dyke does not show any notable difference from other samples confirming that it belongs to the same intrusive suite.

The observed geochemical features are in general comparable with calc-alkaline arc magmas derived from melting of mantle wedge metasomatised by fluids from subducted oceanic slab.

5.2. Lead isotope systematics

5.2.1. Ores

The age corrected lead isotopic compositions of sulfides (n=24) show a range between 17.8 to 19.1 for $^{206}Pb/^{204}Pb$, 37.6 to 38.1 for $^{208}Pb/^{204}Pb$, and 15.50 to 15.61 for $^{207}Pb/^{204}Pb$ (Table 3 and Fig. 5). Six samples representing three sites and three different assemblages of the **Bereznyakovskoe epithermal Au-Ag ore field** establish a very tight isotopic group ($^{206}Pb/^{204}Pb$ 18.001 to 18.040, $^{207}Pb/^{204}Pb$ 15.570 to 15.581, and $^{208}Pb/^{204}Pb$ 37.836 to 37.862 (Fig. 5). Six samples from the **Biksizak base-metal** occurrence also have a very homogeneous lead isotopic composition ($^{206}Pb/^{204}Pb$ 17.894 to 17.987, $^{207}Pb/^{204}Pb$ 15.552 to 15.560, and $^{208}Pb/^{204}Pb$ 37.724 to 37.759). The only sample representing the **Michurino Au-Ag-base-metal** occurrence ($^{206}Pb/^{204}Pb$ = 17.942, $^{207}Pb/^{204}Pb$ = 15.558, $^{208}Pb/^{204}Pb$ = 37.766) plots in the Biksizak field. Two samples representing sub-epithermal style mineralization of the **Birgilda porphyry Cu deposit** have lead isotopic composition similar to the Bereznyakovskoe epithermal Au-Ag ore-field ($^{206}Pb/^{204}Pb$ 18.121 to 18.351, $^{207}Pb/^{204}Pb$ 15.586 to 15.607, $^{208}Pb/^{204}Pb$ 37.976 to 38.096).

The chalcopyrite sample from the **Tomino porphyry copper deposit** differs from Au-Ag and base-metal mineralization in lower ^{207}Pb and ^{208}Pb contents ($^{207}Pb/^{204}Pb$ = 15.517 and $^{208}Pb/^{204}Pb$ = 37.728). The **Kalinovskoe porphyry copper deposit** shows the largest variations in all lead isotopic ratios ($^{206}Pb/^{204}Pb$ 17.8 to 19.1, $^{207}Pb/^{204}Pb$ 15.50 to 15.61, $^{208}Pb/^{204}Pb$ 37.6 to 38.1). The three sulfide samples representing porphyry-style mineralization and located within diorite stock (K-850/176.5, K-850/225.8,

and K-26/236.5) have a relatively narrow range ($^{206}Pb/^{204}Pb$ 17.94 to 18.11, $^{207}Pb/^{204}Pb$ 15.54 to 15.57, $^{208}Pb/^{204}Pb$ 37.92 to 38.12) which is similar to the range established for the other deposits of the ore cluster. Five samples from hosting basalts of the Sargazy Formation are featured by a much wider range of ^{206}Pb and ^{207}Pb ($^{206}Pb/^{204}Pb$ 17.8 to 19.15, $^{207}Pb/^{204}Pb$ 15.5 to 15.61).

5.2.2. Igneous rocks

Lead isotope ratios for the four plagioclase samples from the least altered rocks of the **Birgilda-Tomino Igneous Complex** were corrected for radioactive decay over 430 Ma using U, Th, and Pb contents. Age-corrected lead isotopic compositions ($^{206}Pb/^{204}Pb$ 17.74 to 18.16, $^{206}Pb/^{204}Pb$ 15.49 to 15.58, and $^{208}Pb/^{204}Pb$ 37.63 to 37.89) plot within the field of ore samples (Fig. 5). At that, the lowest lead isotopic ratios were obtained for the post-ore diorite porphyry dyke (Table 3, Fig. 5).

Lead isotope ratios for the three feldspar samples of the **Chelyabinsk Pluton** were corrected for radioactive decay over 355 Ma. They are remarkably different from rocks of the Birgilda-Tomino Igneous Complex and most sulfide samples in higher ^{206}Pb, ^{207}Pb, and ^{208}Pb contents ($^{206}Pb/^{204}Pb$ 15.65 to 15.66, $^{207}Pb/^{204}Pb$ 18.35 to 18.51, and $^{208}Pb/^{204}Pb$ 38.30 to 38.42).

6. Discussion

6.1. Variations in lead isotopic composition in the Birgilda-Tomino ore cluster

On the $^{206}Pb/^{204}Pb$ vs. $^{207}Pb/^{204}Pb$ diagram ore samples of the Birgilda-Tomino ore cluster plot in a wide area between the mantle evolution curve of Zartman and Doe (1981) and the average crustal growth curve of Stacey and Kramers (1975). At that, the lead isotopic ratios of Au-Ag epithermal and base-metal carbonate replacement mineralization types (Bereznyakovskoe, Michurino, Biksizak, and Birgilda) plot within a relatively small field that overlaps the “orogen” evolution curve for 600 to 400 Ma (Fig. 6). The only exception is one pyrite sample from the Birgilda deposit (Bir-3704/71.5) which is shifted to the “upper crust” source.

Lead isotopic ratios of the Kalinovskoe deposit are remarkably different. On the both $^{206}Pb/^{204}Pb$ vs. $^{207}Pb/^{204}Pb$ and $^{206}Pb/^{204}Pb$ vs. $^{208}Pb/^{204}Pb$ diagrams they form a linear trend from the mantle evolution curve to the area of an “anomalous” Pb source. The chalcopyrite sample from the Tomino deposit also fits this trend on the both diagrams.

Plagioclase samples from the Birgilda-Tomino Igneous Complex plot within the same part of the both Pb-Pb diagrams. It is important to note that plagioclase from Bereznyakovskoe and Michurino intrusions are similar in lead isotopic composition with the corresponding deposits. Plagioclase from the Kalinovskoe diorite stock has similar Pb isotopic composition with the Kalinovskoe pyrite samples located in the same stock.

Plagioclase and K-feldspars from the Chelyabinsk pluton plot in the uppermost part of the both

Pb-Pb diagrams; on the $^{206}Pb/^{204}Pb$ vs. $^{207}Pb/^{204}Pb$ plot they fit within the "upper crust" evolution curve (Fig. 6b).

6.2. Identification of lead sources

6.2.1. Anomalous Pb sources

Presence of sulfide samples with anomalous lead isotopic compositions is an important feature of ores from the Kalinovskoe deposit. Negative Pb-Pb model age values (up to –392 Ma) estimated for sulfide samples from the peripheral zones of the deposit in hosting basalts (K-61/127.4, K-57/95.7, K-2270/45.3) point to an excess of radiogenic ^{206}Pb. We expect that other sulfide samples with model ages much younger than Silurian also contain some admixture of radiogenic lead. These are: pyrite and galena samples from the Birgilda deposit with the model ages 221 Ma and 352 Ma; pyrite samples from the Kalinovskoe deposit with model ages 344 Ma to 129 Ma; the chalcopyrite sample from the Tomino deposit with the model age 192 Ma. Average model ages of galena, clausthalite, and altaite samples from the Biksizak, Michurino, and Bereznyakovskoe (432, 429, and 413 Ma respectively) are close to the age of diorites of the Birgilda-Tomino Complex (427 ± 6 Ma) which is supposed to be the age of the deposits and they show no remarkable admixture of radiogenic lead.

The observed admixture may be a result of: (1) mixing line of two distinct types of lead sources during the ore deposition or (2) input of a radiogenic ^{206}Pb in a post-ore phase. The former may be contributed by a fluid with radiogenic lead during the epithermal stage, e.g., a removal of ^{206}Pb from host rocks by meteoric water. This is supported by the presence of epithermal style mineralization (argillic alteration in the Birgilda deposit or Bi sulfosalts in the Kalinovskoe deposit) in samples with radiogenic lead.

The latter possibility is supported by K-Ar ages obtained by Grabezhev et al. (1998) that giving of 325±7 to 298±9 Ma for the Tomino deposit, 313±12 to 268±10 Ma for the Birgilda deposit, 359±9 to 309±10 Ma for the Bereznyakovskoe deposit, and 302±10 to 293±7 Ma for the Biksizak occurrence. This points to a reset of K-Ar system in sericite as a result of heat flow during (1) emplacement of early phases of the Chelyabinsk Pluton (360 to 340 Ma) or (2) formation of the Uralian orogen in the Late Carboniferous to Permian accompanied by emplacement of sub-alkaline phases of the Chelyabinsk Pluton at 275 to 260 Ma (see section 2 for details). Each of these events might have triggered a hydrothermal activity, and presence of mesothermal Au-quartz lodes in the described area support this suggestion. Such hydrothermal activity, though weak and local, could provide an input of radiogenic lead from country rocks. This makes an input of a radiogenic lead in a post-ore phase more reasonable.

Remarkable uranium concentrations reported for Proterozoic metasediment sequences exposed outside of the described area, i.e. 4.8 to 6.7 ppm U on average in different formations as well as basalts of the Sargazy Formation with 4 to 7 ppm U (Puzhakov, 1999) could serve as sources of radiogenic lead

in case of the uranium remobilization due to various hydrothermal and/or tectonomagmatic events. Presence of uneconomic uanium occurrences of infiltration type approx. 60 km to the northwest (Puzhakov et al., 2013), uranium-molybdenum hydrothermal mineralization in relation to to late phases of the Chelyabinsk Pluton about 10 to 15 km to the north of the described area, as well as high uranium concentrations (2.71 to 19.96 ppm) in various phases of the Chelyabinsk Pluton (Fershtater, 2013) indirectly support this suggestion.

6.2.2. Common Pb sources and variations

It can be suggested the initial lead isotope composition of basalt hosting ores of the Kalinovskoe deposit is closed to the sample with the lowest lead isotope ratios, e.g. the sample K-61/124.8 ($^{206}Pb/^{204}Pb$ = 17.782, $^{207}Pb/^{204}Pb$ = 15.503, and $^{208}Pb/^{204}Pb$ = 37.571) with the 441 Ma Pb-Pb model age slightly older than the age to the deposit (Re-Os age of is 430.4±2.0 Ma). Calculated μ_2 = 9.41, ω_2 = 35.5 evidence the mantle source of lead. Similar lead isotope signatures were reported for Early Silurian VHMS Zn-Cu deposits located farther to the north in the Tagil arc (Chernyshev et al., 2008). These are the Early Llandoverian Kaban deposit ($^{206}Pb/^{204}Pb$ = 17.89, $^{207}Pb/^{204}Pb$ 15.53 to 15.54, $^{208}Pb/^{204}Pb$ 37.69 to 37.70 for the main ore stage and $^{206}Pb/^{204}Pb$ = 17.73, $^{207}Pb/^{204}Pb$ = 15.49, $^{208}Pb/^{204}Pb$ = 37.55 for mineralization in the post-ore dyke) and the Late Llandoverian San-Donato deposit ($^{206}Pb/^{204}Pb$ 17.61 to 17.66, $^{207}Pb/^{204}Pb$ 15.46 to 15.47, and $^{208}Pb/^{204}Pb$ 37.36 to 37.35). Taking into account the considered territory is supposed to be either the southern end of the Tagil arc or another arc developed in the same period and on the same oceanic crust (Puchkov, 2016, and references therein), the obtained lead isotopic signatures point to a mantle-derived lead source typical for the described area in the Silurian.

The pyrite sample of the Kalinovskoe deposit located in diorite stock (K-26/236.5) has remarkably higher $^{207}Pb/^{204}Pb$ ratio (15.567) than that located in basalt and is similar to those from the Biksizak and Michurino occurrences (Fig. 6). The latter, in turn is close to the Bereznyakovskoe deposit.

Ore samples of the Biksizak, Michirino, and Bereznyakovskoe deposits have lead isotopic signatures similar to intrusions of the Birgilda-Tomino igneous complex; this confirms genetic relation between epithermal Au-Ag, base-metal carbonate replacement, and porphyry copper mineralization and diorite porphyry intrusions noted earlier (Grabezhev et al., 1998). The common lead source with such isotopic signatures can be identified as a mixed mantle-crustal source. This source could not have been produced in a mature volcanic arc due to mantle differentiation. Most likely was the input of sediments with a crustal lead into the subduction zone, possibly as a result of a denudation of the Proterozoic rocks of the East Uralian microcontinent or the Kazakh continent.

The Sm-Nd systematics of diorite porphyry intrusions of the Birgilda-Tomino Igneous Complex (Grabezhev, 2009) confirms a mantle derived magma source. $\varepsilon(Nd)_i$ of the bulk rock samples makes up 7.0 to 7.5 for the Bereznyakovskoe deposit and 6.5 to 6.7 for the Tomino deposit. This is only slightly

lower than the DMM calculated for 430 Ma as 9.1 (Goldstein and Jacobsen, 1988) and does not support any crustal component. However, the average content of lead in the Primitive mantle is 0.185 ppm (Sun and McDonough, 1989) while in the Upper crust it is up 20 ppm (Taylor and McLennan, 1985), i.e. two orders of magnitude higher. In this case even a small input of crustal material would remarkably change the lead isotopic composition but would be reflected in the Sm-Nd systematics.

The noted difference in lead isotopic composition between ore samples located in andesitic dacite of the Bereznyakovskoe Formation and in basalts of the Sargazy formation point to influence of host rocks. In the hydrothermal system of the Bereznyakovskoe deposit, which represents an upper part of the hypothetical porphyry-epithermal continuum (Grabezhev et al., 1998; Plotinskaya et al., 2014), fluids circulated mainly within the andesitic dacite strata (Fig. 7). In the Michurino and Biksizak systems confined to the base of the andesitic dacite formation and to the underlying limestones, respectively material from basalts of the Sargazy Formation could be involved in the fluid circulation.

6.3.3. General remarks

Porphyry copper deposits formed in intra-oceanic volcanic arc environment often have mantle-derived lead source, e.g. the Hugo Dummett deposit in Mongolia (Dolgopolova et al., 2013), while mantle-crustal mixing trends are common for porphyry deposits formed on continental margins, like the porphyry copper deposits of Arizona (Bouse et al., 1999) or those formed in post-collision setting, e.g. the Sora porphyry Mo deposit (Berzina et al., 2011) or porphyry copper deposits of the Tethyan metallogenic domain (Hou et al., 2011). However, mantle-crustal mixing trend, though smoothed by the radiogenic lead admixture was described for the El Arco porphyry copper deposit, Baja California, linked to a Mesozoic intra-oceanic arc (Weber and Lopez Martinez, 2005) and for the Batu Hijau porphyry copper deposit, Indonesia (Fiorentini and Garwin, 2010).

7. Conclusions

Ore samples have lead isotopic signatures similar to neighboring intrusions of the Birgilda-Tomino Igneous Complex. This confirms genetic relations between epithermal Au-Ag and porphyry copper mineralization and diorite porphyry intrusions.

Lead isotopic ratios for sulfide and plagioclase samples of porphyry and porphyry-related deposits and occurrences of the Birgilda-Tomino ore cluster form a mantle-crustal mixing trend. The Silurian VHMS deposits of the Tagil volcanic arc also fit this trend.

Input of radiogenic ^{206}Pb took place during the post-ore phase as a result of a series of tectono-magmatic events between 360 and 250 Ma, which includes emplacement of at least two phases of the Chelyabinsk Pluton. The latter, however, acted only as a trigger of hydrothermal activity, but not as a lead source.

Acknowledgments

This study is a contribution to IGCP-592 sponsored by IUGS and UNESCO. It was supported by the IGEM RAS basic theme No 72-4, by NHM (via the CERCAMS Fellowship Program), and by the Russian Foundation for Basic Research, Projects NN 14-05-00725 and 16-05-00622. We would like to thank the staff or the Russian Copper Company and the YuzhUralZoloto Company for assistance during the fieldwork. T.A. Osipova (Zavaritsky Institute of Geology and Geochemistry, Yekaterinburg) is thanked for providing samples of the Chelyabinsk pluton. A.I. Yakushev and Ya.V. Bychkova (IGEM RAS) are thanked for the XRF and ICP-MS analyses respectively. We would like to express our gratitude to Dr. A. Yakubchuk for his critical comments and efforts of revising the English language. Review by M. Porter helped to improve the paper. Prof. V. Maslennikov is thanked for constructive comments and for the editorial handling.

References

Bea, F., Fershtater, G.B., Montero, P. 2002. Granitoids of the Uralides: Implication for the Evolution of the Orogen. Mountain building in the Uralides: Pangea to the present. Geophysical Monograph. 132. Copyright by the American Geophysical Union. pp 211–232.

Berzina, A.P., Berzina, A.N., Gimon, V.O., Krymskii, R.Sh., 2011. Isotopy of lead from the Sora porphyry Cu-Mo magmatic center (Kuznetsk Alatau). Russ. Geol. Geophys. 52, 493-502

Bouse, R.M., Ruiz, J., Titley, S.R., Tosdal, R.M., Wooden, J.L., 1999. Lead isotope compositions of Late Tertiary igneous rocks and sulfide minerals in Arizona: implications for the sources of plutons and metals in porphyry copper deposits. Econ. Geol. 94, 211-244.

Chernyshev, I.V., Chugaev. A.V., Shatagin, K.N., 2007. High-precision Pb isotope analysis by multicollector-ICP-mass-spectrometry using $^{205}Tl/^{203}Tl$ normalization: Optimization and calibration of the method for the studies of Pb isotope variations. Geochem. Int. 45, 1065-1076.

Chernyshev, I.V., Vikent'ev, I.V., Chugaev, A.V., Shatagin, K.N., Moloshag, V.P., 2008. Sources of material for massive sulfide deposits in the Urals: evidence from the high-precision MC–ICP–MS isotopic analysis of Pb in Galena. Dokl. Earth Sci. 418, 178–183.

Chugaev. A.V., Chernyshev, I.V., Lebedev, V.A., Eremina, A.V., 2013. Lead Isotope composition and origin of the quaternary lavas of Elbrus Volcano, the Greater Caucasus: High-precision MC-ICP-MS data. Petrology 21, 16-27.

Doe, B.R., Zartman, R.E. 1979. Plumbotectonics. In: Barnes, H.L. (eds) Geochemistry of hydrothermal ore deposits, 3rd edn. Wiley, New York, pp 22–70

Dolgopolova, A., Seltmann, R., Armstrong, R., Belousova, E., Pankhurst, R.J., Kavalieris, I., 2013. Sr–Nd–Pb–Hf isotope systematics of the Hugo Dummett Cu–Au porphyry deposit (Oyu Tolgoi, Mongolia). Lithos 164–167, 47–64.

Fedoseev, V.V., 2007. Raw input sources of the Yuzhuralzoloto Ltd. in the Chelyabinsk area. Mineral Resourses of Russia, Economy and Management 9, 20–27 (in Russian).

Fershtater, G.B., 2013. Palaeozoic intrusive magmatism of the Middle and South Urals**.** Ural Branch of RAS, Yekaterinburg (in Russian).

Fiorentini, M.L., Garwin, S.L., 2010. Evidence of a mantle contribution in the genesis of magmatic rocks from the Neogene Batu Hijau district in the Sunda Arc, South Western Sumbawa, Indonesia. Contrib. Mineral. Petrol. 159, 819–837.

Goldstein, S.J., Jacobsen, S.B., 1988. Nd and Sr isotopic systematic of river water suspended material: implications for crustal evolution. Earth Plan. Sci. Letters 87(3), 249-265.

Grabezhev, A.I., 2009. Sr–Nd–C–O–H–S isotope-geochemical description of South Urals porphyry-copper fluid-magmatic systems: probable sources of matter. Lithosphera 6, 66–89 (in Russian with English abstract).

Grabezhev, A.I., Kuznetsov, N.S., Puzhakov, B.A., 1998. Ore and Alteration Zoning of Sodium Type Copper-Porphyry Column (Paragonite-Bearing Aureoles, the Urals). IGG Publisher, Yekaterinburg (in Russian).

Grabezhev, A.I., Bea, F., Montero, M.P., Fershtater, G.B., 2013. The U–Pb SHRIMP age of zircons from diorites of the Tomino–Bereznyaki ore field (South Urals, Russia): evolution of porphyry Cu–epithermal Au–Ag system. Russ. Geol. Geophys. 54, 1332–1339.

Grabezhev, A.I., Sazonov, V.N., Murzin, V.V., Moloshag, V.P., Sotnikov, V.I., Kuznetsov, N.S., Pyzhakov, B.A., Pokrovsky, B.G., 2000. The Bereznyakovsk gold deposit (South Urals, Russia). Geol. Ore Deposit. 42, 33–46.

Hou, Z., Zhang. H., Pan,X., Yang, Z., 2011. Porphyry Cu (-Mo-Au) deposits related to melting of thickened mafic lower crust: Examples from the eastern Tethyan metallogenic domain. Ore Geol. Rev. 39, 21–45.

Kallistov, G.A., 2014. Duration and stages of emplacement of the Chelyabinsk granitoid batholith. IGG UrB RAS Yearbook-2013, *161,* 343–349 (in Russian).

Lehmann, B.J., Heinhorst, J., Hein, U., Neumann, M., Weisser, J.D., Fedosejev, V.V., 1999. The Bereznjakovskoe gold trend, southern Urals, Russia. Miner. Deposita 34, 241–249.

Osipova, T.A., Kallistov, G.A., Travin, A.V., Dril, S.I., 2010. The first data about the Mesozoic granitoids in Chelyabinsk pluton (the South Urals). Lithosphera 4, 163–169 (in Russian with English abstract).

Pearce, J.A., Peate, D.W., 1995. Tectonic implications of the composition of volcanic arc magmas: Annu. Rev. Earth Pl. Sc. 23, 251–285.

Plotinskaya, O.Yu., Grabezhev, A.I., Seltmann, R., 2015. Fahlores Compositional Zoning in a Porphyry–Epithermal System: Biksizak Occurrence, South Urals, Russia as an Example. Geol. Ore Deposit. 57, 42−63.

Plotinskaya, O.Yu., Groznova, E.O., Grabezhev, A.I., Novoselov, K.A., 2010. Mineralogy and Formation Conditions of Ore from the Biksizak Silver–Base Metal Occurrence of the South Urals in Russia. Geol. Ore Deposit. 52, 392–409.

Plotinskaya, O.Yu., Groznova, E.O., Kovalenker, V.A., Novoselov, K.A., Seltmann, R., 2009. Mineralogy and formation conditions of ores in the Bereznyakovskoe ore field, the Southern Urals, Russia. Geol. Ore Deposit. 51, 371–397.

Plotinskaya, O.Yu., Grabezhev, A.I., Groznova, E.O., Seltmann, R., Lehmann, B., 2014. The Late Paleozoic porphyry-epithermal spectrum of the Birgilda−Tomino ore cluster in the South Urals, Russia. J. Asian Earth Sci. 79, 910−931.

Plotinskaya, O.Y., Grabezhev, A.I., Tessalina, S., Seltmann, R., Groznova, E.O., Abramov, S.S., 2016. Porphyry deposits of the Urals: geological framework and metallogeny. Ore Geol. Rev. DOI:10.1016/j.oregeorev.2016.07.002

Puchkov, V.N., 2016. General features relating to the occurrence of mineral deposits in the Urals: What, where, when and why. Ore Geol. Rev. doi:10.1016/j.oregeorev.2016.01.005

Puzhakov, B.A., 1999. Productive granitoids, metasomatism, and mineralization of the Birgil'da–Tomino ore cluster, Cand. Sci. (Geol.–Mineral.) Thesis, Yekaterinburg (in Russian).

Puzhakov, B.A., Savel'ev, V.P., Kuznetsov, N.S., Shokh, V.D., Shhul'kin, E.P., Shhul'kina, N.E., Zhdanov, A.V., Dolgova, O.Ya., Tarelkina, E.A., Orlov., M.V., 2013. State geological map of the Russian Federation. 1:1 000 000 scale (third generation). The Uralian series. Sheet N-41–Chelyabinsk. Explanatory note. VSEGEI publisher. 415p. (in Russian).

Romashova, L.N., 1984. The Birgildinskoe porphyry copper deposit. Geol. Ore Dep. 26(2), 20–31 (in Russian).

Seravkin, I.B., Snachev, V.I., 2012. Stratiform base-metal deposits in the Eastern province of the Southern Urals, Russia. Geol. Ore Deposit. 54, 209–218.

Samygin, S.G., Burtman, V.S., 2009. Tectonics of the Ural Paleozoides in comparison with the Tien Shan. Geotectonics 43, 133−151.

Sillitoe, R.H., 2010. Porphyry copper systems. Econ. Geol. 105, 3−41.

Snachev, V.I., Kuznetsov, N.S., 2011. Gold deposits of the gold-sulfide-quartz type of the Chelyabinsk ore area. Geological Digest 9, 201−207. (in Russian).

Snachev, A.V., Puchkov, V.N., Saveliev, D.E., Snachev, V.I., 2006. Geology of the Aramil-Sukhtelinsk Zone of the Urals. Design Poligraph Service, Ufa (in Russian).

Spadea, P., d'Antonio, M., 2006. Initiation and evolution of intra-oceanic subduction in the Uralides: geochemical and isotopic constrains form Devonian oceanic rocks of the Southern Urals, Russia. Island Arc 15, 7–25.

Stacey, J.S., Kramers, J.D. 1975. Approximation of terrestrial lead isotope evolution by a two stage model. Earth Planet. Sci. Lett. 26, 207–221.

Sun, S.S., McDonough, W.F., 1989. Chemical and isotopic systematics of oceanic basalts: implications for mantle compositions and processes. In: Saunders, A.D.,Norry, M.J. (eds.): Magmatism in the ocean basins. Geol. Soc. Long. Spec. Publ. 42, 313–345.

Taylor, S.R., McLennan, S.M., 1985. The continental crust: its composition and evolution: an examination of the geochemical record preserved in sedimentary rocks. Blackwell Scientific 312p.

Tessalina, S.G., Herrington, R.J., Taylor, R.N., Sundblad K., Maslennikov, V.V., Orgeval, J.-J., 2016. Lead isotopic systematics of massive sulphide deposits in the Urals: Applications for geodynamic setting and metal sources. Ore Geol. Rev. 72, 22–36.

Tevelev, A.V., Kosheleva, I.A., Popov, V.S., Kuznetsov, I.E., Osipova, T.A., Pravikova, N.V., Vostretsova, E.S., Gustova, A.S., 2006. Paleozoic rocks of the East-Uralian and Trans-Uralian conjunction zone. MSU publ., Moscow (in Russian).

Vinogradov, A.P., Tarasov, L.S., Zikov, C.I., 1960. Lead isotopic composition of Urals volcanogenic massive sulphide deposits. Geochemistry 6, 475–489 (in Russian).

Volchkov, A.G., Kuznetsov, V.V., Nikeshin, Yu.V., 2015. Tasks and targets of the national budget funded geological exploration for base metals (Cu, Pb, Zn). Rudy i Metally (1) 30–35 (in Russian with English abstract).

Weber, B., Lopez Martinez, M., 2005. Pb, Sr, and Nd isotopic and chemical evidence for a primitive island arc emplacement of the El Arco porphyry copper deposit (Baja California, Mexico). Miner. Deposita 40, 707-725.

Yazeva, R.G., Bochkarev, V.V., 1995. Silurian Island Arc of the Urals: Structure, Evolution, and Geodynamics, Geotectonics, English translation. 29(6), 478–489.

Yazeva R.G., Bochkaryov, V.V., 1998. Geology and geodynamics of the Southern Urals (the experience of geodynamical mapping). Yekaterinburg: Uralian branch RAS. 204p. (in Russian with English abstract).

Zartman, R.E., Doe, B.R., 1981. Plumbotectonics—the model. Tectonophysics 75, 135–162.

Fig. 1. Simplified geology of the Birgilda–Tomino ore cluster (modified after Grabezhev et al., 2000). The shaded area on the inset shows the East Uralian volcanic terrane.

Fig. 2. Representative samples from epithermal Au-Ag (a to d), base-metal (e) and porphyry copper (f to i) mineralization selected for Pb isotope study. SEI- secondary electron image, f- hand specimen, others - reflected light microphotographs.

a–c –Bereznyakovskoe ore field: a– inclusions of selenoan galena (Gn) and tennantite (Tn) in enargite (En), sample Br-17/05; b– inclusions of altaite (Alt) in tennantite, sample Br-3/05; c– galena-sphalerite stage, galena, sphalerite (Sp), tetrahedrite (Tt) and pyrite in quartz-carbonate matrix, sample Br-10/108.3; d– Michurino occurrence, galena in chalcopyrite (Ccp), sample Z-201/79.4; e– Biksizak occurrence, galena inclusions in quartz (Qtz), sample BS-49/358.5; f– the Tomino deposit, chalcopyrite nests in quartz veinlet, sample T-3501/120.5; g– Birgilda deposit, base-metal assemblage in argillisite, sample Bir-4703/134; h–i: Kalinovskoe deposit: h– minerals of bismuthinite-aikinite series (Bi-Aik) in chalcopyrite, sample K-2270/45.3; i– selenoan galena and Ag selenides in bornite (Bn), sample K-61/124.8.

Fig. 3. Magmatic rocks selected for Pb isotope analysis, hand specimens.

(a) to (d) – Birgilda-Tomino Igneous Complex: a– quartz diorite porphyry, Bereznyakovskoe deposit, sample Br-120A01/159; b– quartz diorite porphyry, Michurino occurrence sample Z-105/89.8; c– diorite, Kalinovskoe deposit, sample K-61/156; d– post-ore diorite porphyry dyke, Kalinovskoe deposit, sample K-4/230; (e) to (g)– Chelyabinsk Pluton: e– quartz diorite, sample ChlB-1, f– granodiorite, sample Chl–395, g– biotite granite, sample Chl–304.

Fig. 4. Primitive mantle normalized spider diagram (a) and chondrite normalized REE spectra (b) for rocks of the Birgilda-Tomino Igneous Complex selected for Pb isotopic studies. (normalized after Sun and McDonough, 1989; Taylor and McLennan, 1985). The early phases of the Chelyabinsk Pluton are shown by a shaded area (data derived from Fershtater, 2013).

Fig. 5. Age-corrected lead isotope compositions of sulfides and feldspars of the Birgilda-Tomino ore cluster; numbers correspond to those in Table 1. (a) $^{208}Pb/^{204}Pb$ vs $^{206}Pb/^{204}Pb$ plot, (b) $^{207}Pb/^{204}Pb$ vs $^{206}Pb/^{204}Pb$ plot.

Pl– plagioclase, Kfs– K-feldspar.

Fig. 6. $^{207}Pb/^{204}Pb$ vs $^{206}Pb/^{204}Pb$ plot for sulfides and feldspars of the Birgilda-Tomino ore cluster

compared with Stacey and Kramers (1975) model growth curve (S-K) and Doe and Zartman (1979) growth curves for mantle and upper crust. Samples with anomalous Pb are white, others are colored.

Fig. 7. Position of the deposits of the Birgilda–Tomino ore cluster in the hypothetical stratigraphic column of the studied area (modified after Grabezhev et al., 2000), and $^{207}Pb/^{204}Pb$ and $^{208}Pb/^{204}Pb$ histograms in ore and rock samples. Arrows show fluid circulation, see Fig. 1 for legend of the column.

Table 1. Ore and rock samples selected for lead isotope analysis

No	Sample No	Sample description
Ore samples		
Yuzhnoe Au-Ag deposit		
1	Br-10/108.3	Galena-sphalerite stage. Stringer of **galena** and sphalerite (Fig. 2c).
Bereznyakovskoe Au-Ag deposit		
2	Br-17/05	Main ore stage. Massive enargite with inclusions of tennantite, Sn sulfosalts, and Se-bearing **galena** (Fig. 2a)**.**
3	Br-3/05	Main ore stage. Massive tennantite with minor quartz, pyrite, Au-Ag tellurides, and **altaite** (Fig. 2b)**.**
4	Br-6/10	Galena-sphalerite stage. Pinkish quartz veinlet with 1cm **galena** nest
Deputatskoe Au-Ag deposit		
5	Br-13213/82.3	Galena-sphalerite stage. Pinkish quartz veinlet with rare nests of **galena**
6	Br-13172/98.2	Galena-sphalerite stage. Carbonate veinlet with nests (up to 1 cm) of **galena** and sphalerite.
Michurino Au-Ag-base-metal occurrence		
7	Z-201/79.4	Massive pyrite aggregate (crystals up to 0.5 cm) cut and brecciated by carbonate veinlet with chalcopyrite, minor tennantite and galena (Fig. 2f).
Biksizak base-metal occurrence		
8	BS-50/320	Massive pyrite ore with carbonate stringers.
9	BS-49/358.5	Massive pyrite ore with minor sphalerite and galena (fig. 2e).
10	BS-49/361.2	Veinlet filled with pyrite, **galena**, chalcopyrite in altered limestone.
11	BS-5/257	Massive pyrite ore.
12	BS-44/292	Massive pyrite ore with **galena**, sphalerite, fahlore, tellurides, and native gold filling pores and cracks.
13	BS-41/333.2	**Western site of the occurrence**. Massive pyrite ore with pyrite-sphalerite veinlet.
Birgilda porpyry copper deposit		
14	Bir-3704/71.5	Diorite porphyry with intense phyllic alteration; grey quartz veinlet overlapped with carbonate and pyrite.
15	Bir-4703/134	Quartz-carbonate veinlet with chalcopyrite, **galena**, minor sphalerite and pyrite, accompanied by argillic alteration (Fig. 2g).
Tomino porpyry copper deposit		
16	T-3501/120.5	White quartz veinlet with abundant chalcopyrite and minor pyrite (Fig. 2f).
Kalinovskoe porpyry copper deposit		
17	K-850/176.5	Veinlet of gray quartz with massive pyrite in diorite porphyry.
18	K-850/225.8	Veinlet of gray quartz with pyrite in selvages in diorite porphyry.
19	K-26/236.5	White carbonate veinlet with pyrite in diorite porphyry.
20	K-61/96.8	Basalt with pyrite metacrysts.
21	K-61/124.8	Basalt with white quartz veinlet with 1 cm bornite; bornite contains micron-scale inclusions of gold, tellurides and selenides (Fig. 2i).
22	K-61/127.4	Basalt with pervasive biotite and minor chlorite alteration and chalcopyrite (1 to 3 cm).
23	K-57/95.7	Gray quartz veinlet with up to 0.5cm bornite and chalcopyrite.
24	K-2270/45.3	Basalt with intense chlorite-sericite alteration and up to 5cm chalcopyrite ; chalcopyrite contains inclusions of Bi and **Pb sulfosalts** (Fig. 2h).
Rocks of the Birgilda-Tomino Igneous Complex		
25	Br-120A01/159.5	Quartz diorite porphyry, Yuzhnoe deposit (Fig. 3a)
26	Z -105/89.8	Quartz diorite porphyry, Michurino occurrence (Fig. 3b)
27	K-61/156	Diorite , Kalinovskoe deposit (Fig. 3c)

28	K-4/230	Post-ore diorite porphyry, Kalinovskoe deposit (Fig. 3d)
Rocks of the Chelyabinsk Pluton		
29	Chl-B-1	Quartz diorite (Fig. 3e)
30	Chl -395	Granodiorite (Fig. 3f)
31	Chl-B-4	Biotite granite(Fig. 3g)

Table 2. Chemical composition of rocks of the Birgilda-Tomino Igneous Complex selected for Pb isotopic studies

Sample No	120A01/159.5	Z-105/89.8	K-61/156	K-4/230
Na_2O	4.98	3.94	5.92	6.07
MgO	5.26	4.52	3.17	3.26
Al_2O_3	18.37	17.43	18.02	18.43
SiO_2	58.64	55.36	57.96	58.90
K_2O	1.37	0.88	0.78	0.86
CaO	0.77	5.15	7.34	2.89
TiO_2	0.36	0.31	0.38	0.42
MnO	0.451	0.192	0.052	0.087
Fe_2O_3	5.31	5.26	3.43	5.55
P_2O_5	0.08	0.08	0.12	0.10
S	0.55	<0.02	<0.02	0.14
LOI	4.25	6.73	2.69	3.32
Cr	50	72	10	11
V	159	125	108	118
Co	21	14	12	11
Ni	15	17	8	11
Cu	41	31	97	5
Zn	165	344	29	79
Rb	10	13	9	9
Sr	191	163	453	318
Zr	55	62	50	64
Ba	268	126	137	168
As	117	<5	<5	<6
Li	18	10	4.6	7.1
Be	0.51	0.50	0.76	0.60
Sc	31	29	26	32
Y	5.0	3.9	9	5.7
Nb	1.1	0.76	1.3	1.3
Mo	0.59	0.82	1.9	1.5
Ag	2.6	0.51	0.47	0.83
Cd	0.18	0.33	0.45	0.20
Sn	<d.l.	<d.l.	0.54	<d.l.
Cs	0.67	0.49	0.63	0.52
La	14	3.7	5.8	9.5
Ce	28	8.9	15	20
Pr	3.6	1.1	2.2	2.6
Nd	13.18	4.6	9.4	10.62
Sm	2.3	0.94	2.0	2.1
Eu	0.71	0.34	0.87	0.78

Gd	3.0	1.2	2.3	2.7
Tb	0.31	0.16	0.33	0.32
Dy	1.2	0.83	1.6	1.4
Ho	0.23	0.17	0.33	0.25
Er	0.80	0.60	1.0	0.83
Tm	0.11	0.09	0.14	0.11
Yb	0.77	0.73	0.99	0.86
Lu	0.13	0.12	0.14	0.13
Hf	1.8	2.1	1.5	2.8
Ta	<d.l.	<d.l.	<d.l.	<d.l.
W	0.86	0.33	1.7	0.30
Pb	4.9	2.7	14.05	7.9
Bi	<d.l.	<d.l.	0.13	0.068
Th	1.1	0.95	0.70	1.3
U	0.62	0.62	0.49	0.52

LOI- loss on ignition, d.l.- detection limit.

Table 3. U, Th, Pb elemental and Pb isotopic composition of ores of the Birgilda-Tomino ore cluster

№	Sample No	Mineral	Pb isotope values			Pb, ppm	Th, ppm	U, ppm	Corrected Pb isotope values			μ_2	ω_2	T_m
			$^{206}Pb/^{204}Pb$	$^{207}Pb/^{204}Pb$	$^{208}Pb/^{204}Pb$				$^{206}Pb/^{204}Pb$	$^{207}Pb/^{204}Pb$	$^{208}Pb/^{204}Pb$			
Yuzhnoe Au-Ag deposit														
1	Br-10/108.3	galena	18.0186	15.5810	37.8618	n.a.	n.a.	n.a.	–	–	–	9.70	36.90	419
Bereznyakovskoe Au-Ag deposit														
2	Br-3/05	altaite	18.0402	15.5742	37.8547	n.a.	n.a.	n.a.	–	–	–	9.61	36.90	429
3	Br-6/10	galena	18.0169	15.5800	37.8564	n.a.	n.a.	n.a.	–	–	–	9.68	36.80	414
4	Br-17/05	galena-clausthalite	18.0468	15.5704	37.8502	147	0.14	0.56	18.030	15.570	37.850	9.64	36.50	386
Deputatskoe Au-Ag deposit														
5	Br-13213/82.3	galena	18.0154	15.5742	37.8383	n.a.	n.a.	n.a.	–	–	–	9.67	36.6	407
6	Br-13172/98.2	>>	18.0006	15.5759	37.8359	n.a.	n.a.	n.a.	–	–	–	9.68	36.7	422
Michurino ocurrence														
7	Z-201/79.4	>>	17.9424	15.5575	37.7659	n.a.	n.a.	n.a.	–	–	–	9.61	36.4	429
Biksizak base-metal occurrence														
8	BS-50/320	pyrite	17.9600	15.5524	37.7241	77	0.030	0.16	–	–	–	9.58	35.9	405
9	BS-49/358.5	>>	17.9282	15.5551	37.7433	198	0.25	0.39	–	–	–	9.61	36.4	435
10	BS-49/361.2	galena	17.9163	15.5554	37.7481	n.a.	n.a.	n.a.	–	–	–	9.61	36.6	455
11	BS-5/257	pyrite	17.9092	15.5525	37.7574	757	0.23	0.54	–	–	–	9.60	36.5	444
12	BS-44/292	galena	17.8942	15.5516	37.7272	n.a.	n.a.	n.a.	–	–	–	9.60	36.5	454
13	BS-41/333.2	pyrite	18.0307	15.5628	37.7596	716	0.15	6.38	17.987	15.560	37.759	9.61	36.1	401
Birgilda porphyry copper deposit														
14	Bir-3704/71.5	pyrite	18.3687	15.608	38.1160	8.7	0.23	0.080	18.351	15.607	38.096	9.72	36.2	221
15	Bir-4703/134	galena	18.1212	15.586	37.9755	n.a.	n.a.	n.a.	–	–	–	9.69	36.8	352
Tomino porphyry copper deposit														
16	T-3501/120.5	chalcopyrite	18.1390	15.517	37.7284	4.4	0.077	0.035	–	–	–	9.38	34.0	192
Kalinovskoe porphyry														

copper deposit														
17	K-850/176.5	pyrite	18.1407	15.546	38.1403	20	0.39	0.15	18.114	15.544	38.120	9.50	36.8	270
18	K-850/225.8	>>	18.006	15.540	37.917	21	0.19	0.050	–	–	–	9.51	36.4	344
19	K-26/236.5	>>	17.9398	15.567	37.946	4.2	0.073	0.030	–	–	–	9.65	37.6	449
20	K-61/96.8	>>	18.3611	15.567	37.7619	4.6	0.18	0.042	–	–	–	9.55	33.6	129
21	K-61/124.8	galena-clausthalite	17.7984	15.504	37.5999	18	0.46	0.11	17.782	15.503	37.571	9.41	35.5	441
22	K-61/127.4	pyrite, chalcopyrite	19.1676	15.610	37.7441	8.7	0.32	0.081	19.148	15.609	37.701	9.58	29.4	-392
23	K-57/95.7	chalcopyrite	18.5776	15.580	37.8126	13	0.20	0.10	18.560	15.579	37.806	9.56	32.7	2
24	K-2270/45.3	bismithine-aikinite	19.3053	15.614	37.7246	5.5	0.10	0.18	19.036	15.599	37.724	9.56	29.9	-327

T_m=model age, $\mu=^{238}U/^{204}Pb$, $\omega=^{232}Th/^{204}Pb$ (Stacey and Kramers, 1975); n.a.— not analyzed; initial $^{206}Pb/^{204}Pb$, $^{207}Pb/^{204}Pb$, and $^{208}Pb/^{204}Pb$ values were recalculated for 430Ma

Table 4. U, Th, Pb elemental and Pb isotopic composition of feldspars from diorites of the Birgilda-Tomino Igneous Complex and the Chelyabinsk Pluton, corrected for U decay over 430 Ma and 355 Ma, respectively.

No	Sample No	Mineral	Pb isotope values			Pb, ppm	Th, ppm	U, ppm	Corrected Pb isotope values		
			$^{206}Pb/^{204}Pb$	$^{207}Pb/^{204}Pb$	$^{208}Pb/^{204}Pb$				$^{206}Pb/^{204}Pb$	$^{207}Pb/^{204}Pb$	$^{208}Pb/^{204}Pb$
Birgilda-Tomino Igneous Complex											
25	Br-120A01/159.5	Plagioclase	18.331	15.5897	38.1197	1.0	0.17	0.035	18.157	15.580	37.886
26	Z-105/89.8	>>	18.0718	15.5575	37.8776	2.0	0.24	0.021	18.021	15.555	37.713
27	K-61/156	>>	18.1614	15.5454	37.7656	1.1	0.11	0.034	18.007	15.537	37.627
28	K-4/230	>>	17.8235	15.4941	37.6862	2.0	0.086	0.033	17.745	15.490	37.628
Early phases of the Chelyabinsk Pluton											
29	Chl B-1	Plagioclase	18.3905	15.6516	38.3103	16	0.12	0.12	18.360	15.650	38.302
30	Chl-395	K feldspar	18.5218	15.6626	38.4230	54	0.1	0.19	18.507	15.662	38.421
31	Chl B-4	>>	18.3788	15.655	38.3449	64	1.6	0.41	18.353	15.654	38.316

Fig. 1

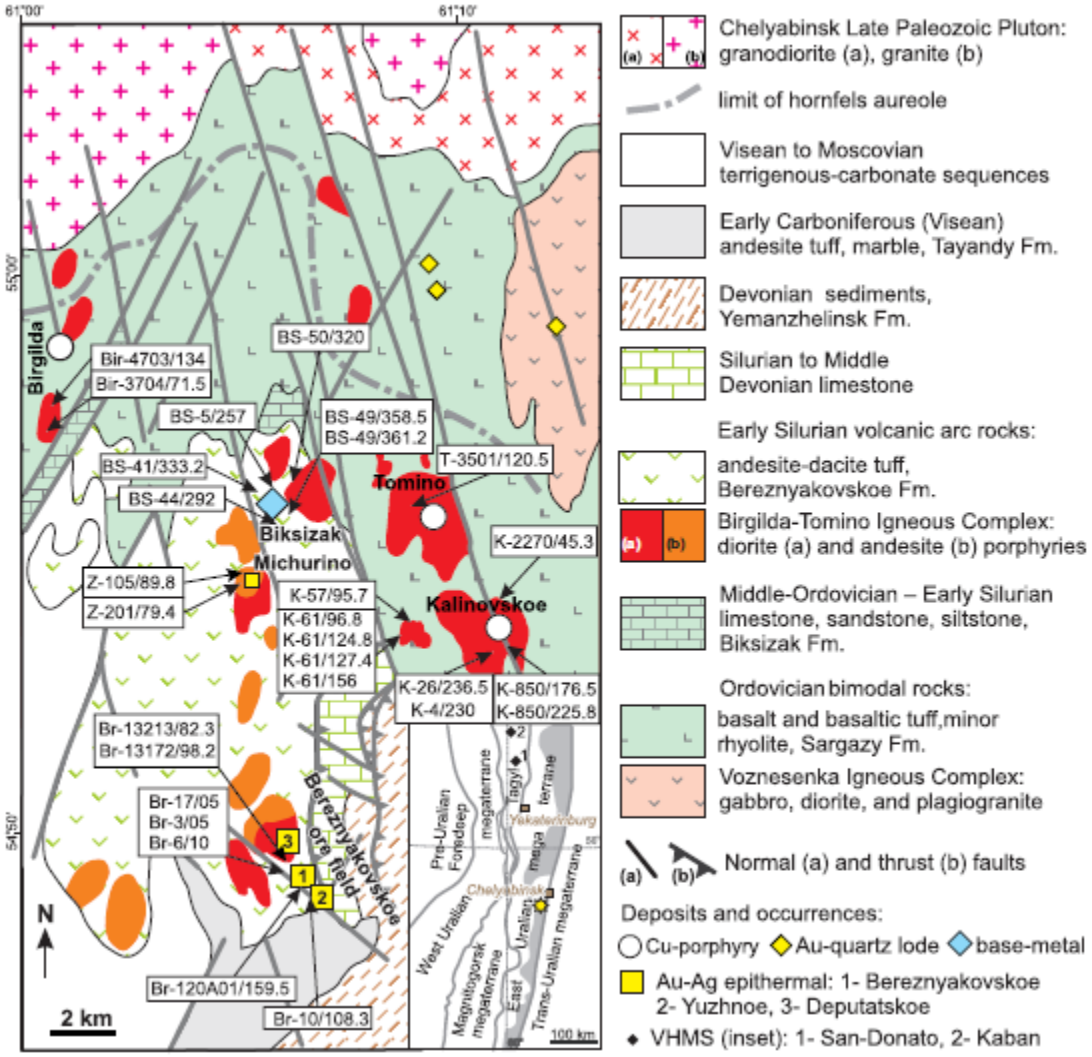

Fig. 2

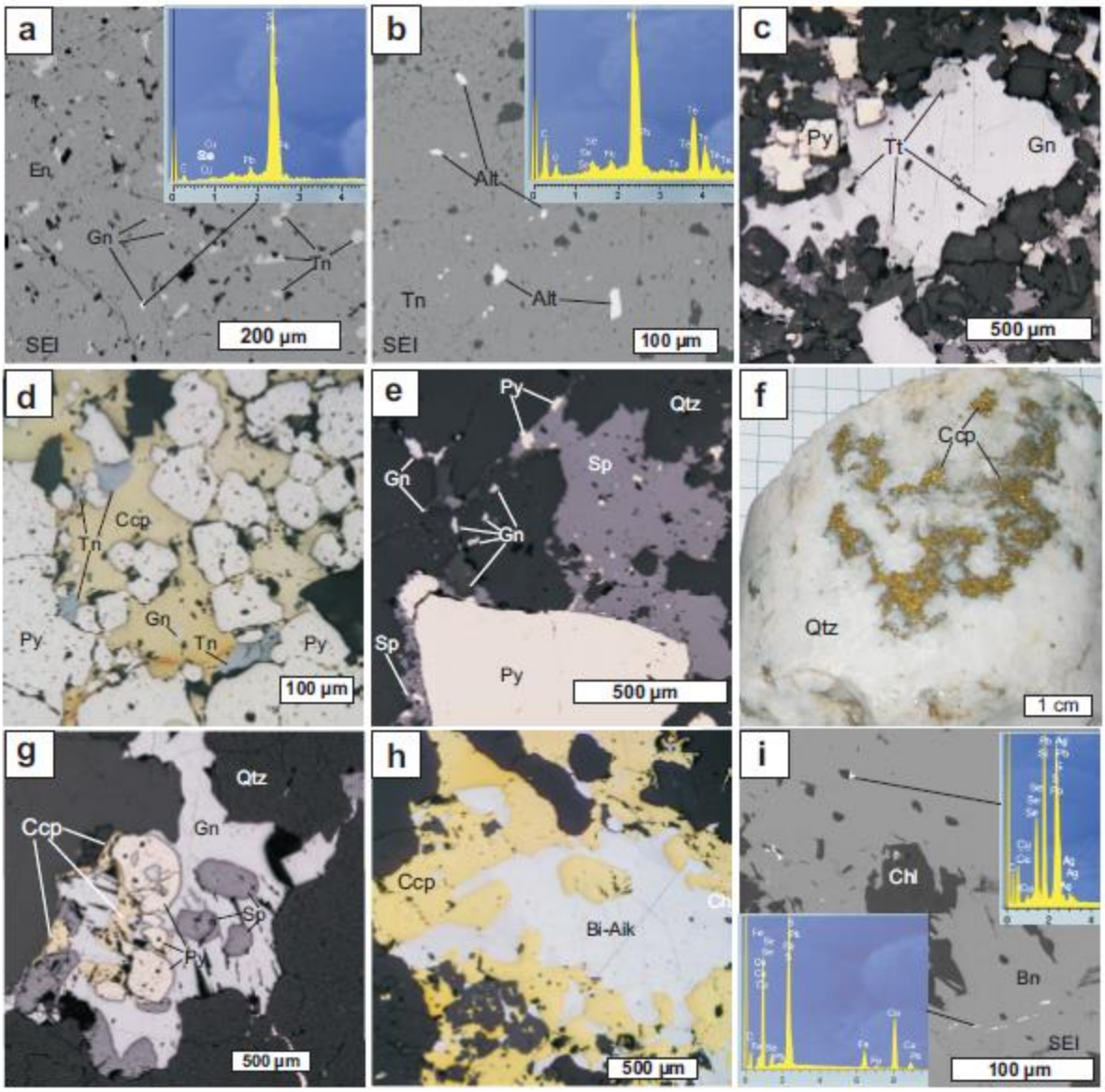

Fig. 3

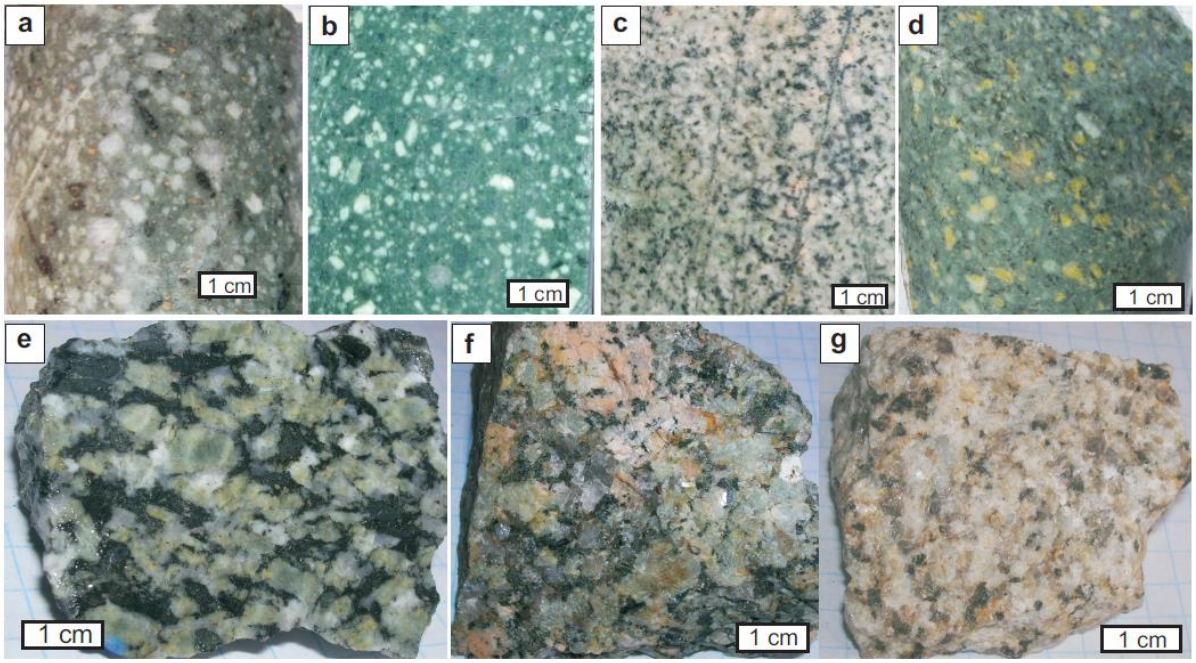

Fig. 4

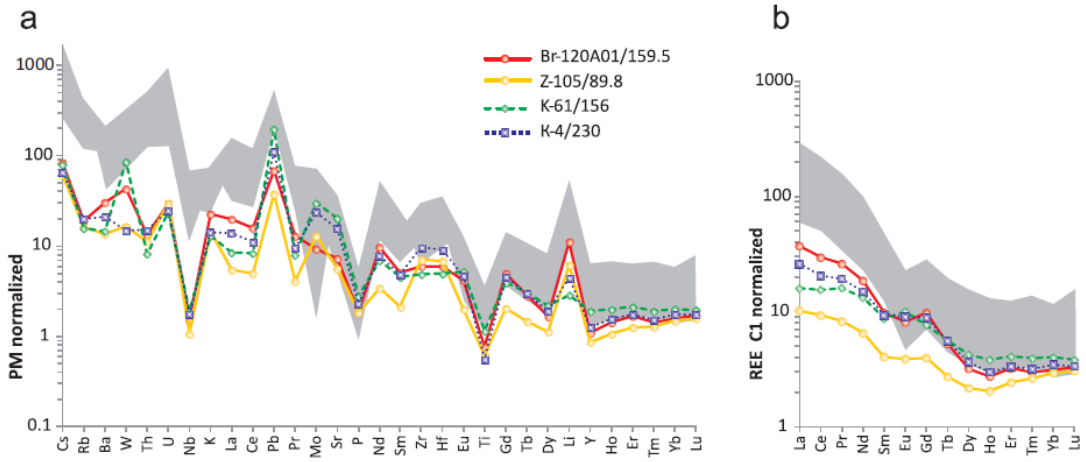

Fig. 5

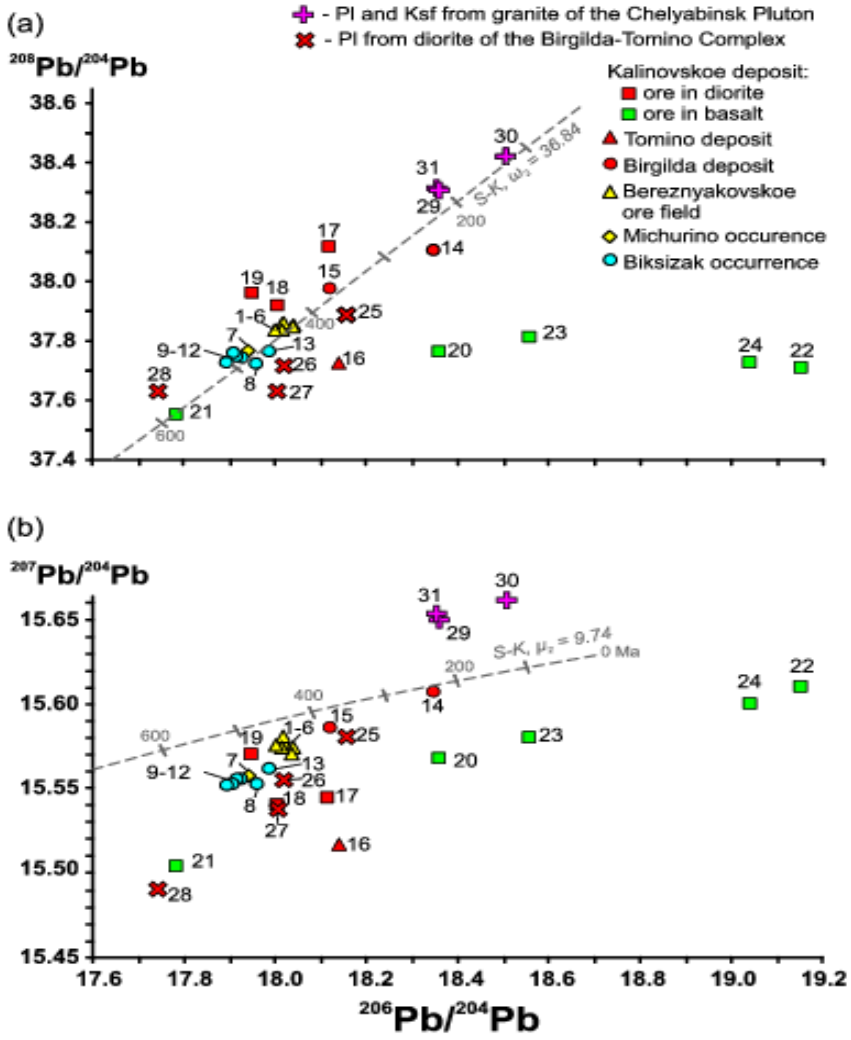

Fig. 6

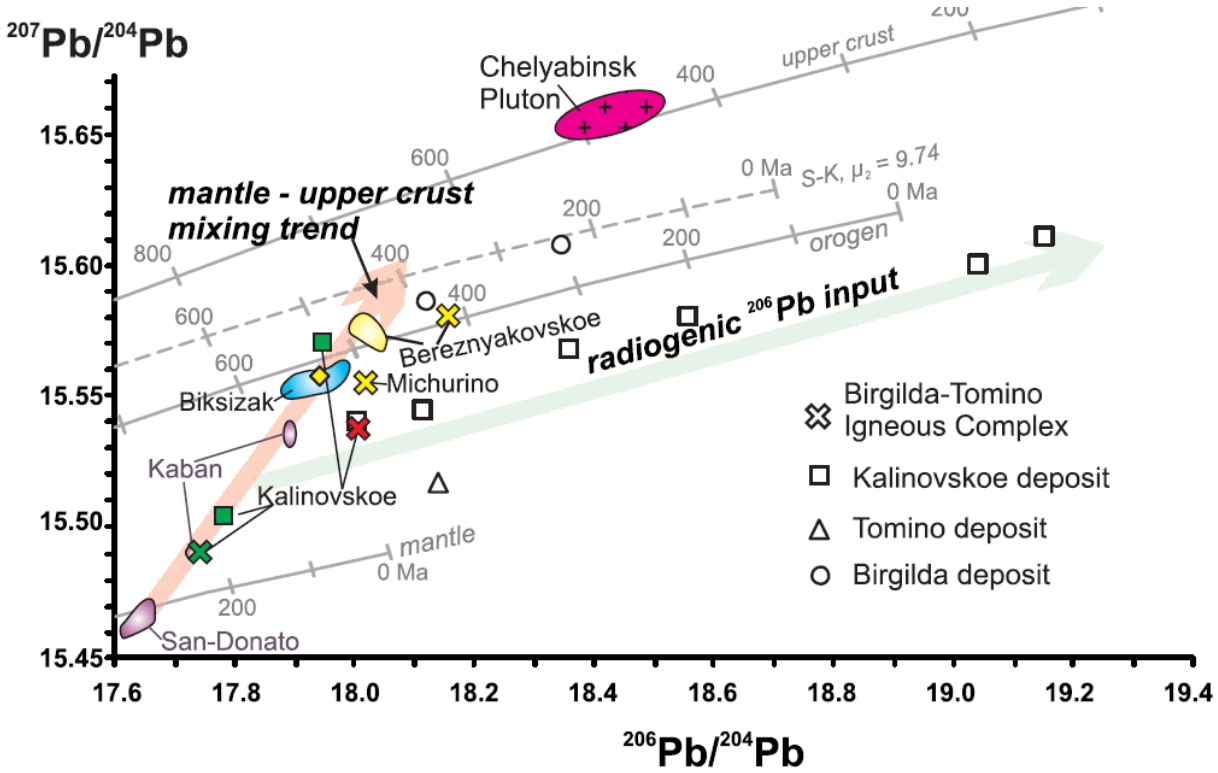

Fig. 7

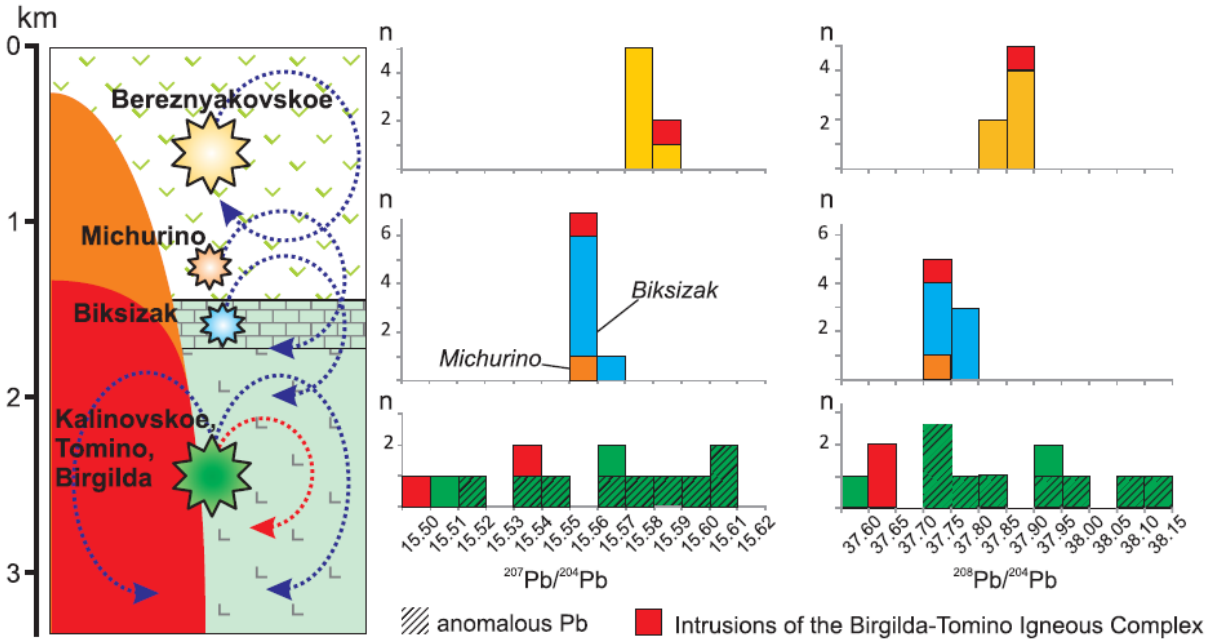

Graphical abstract

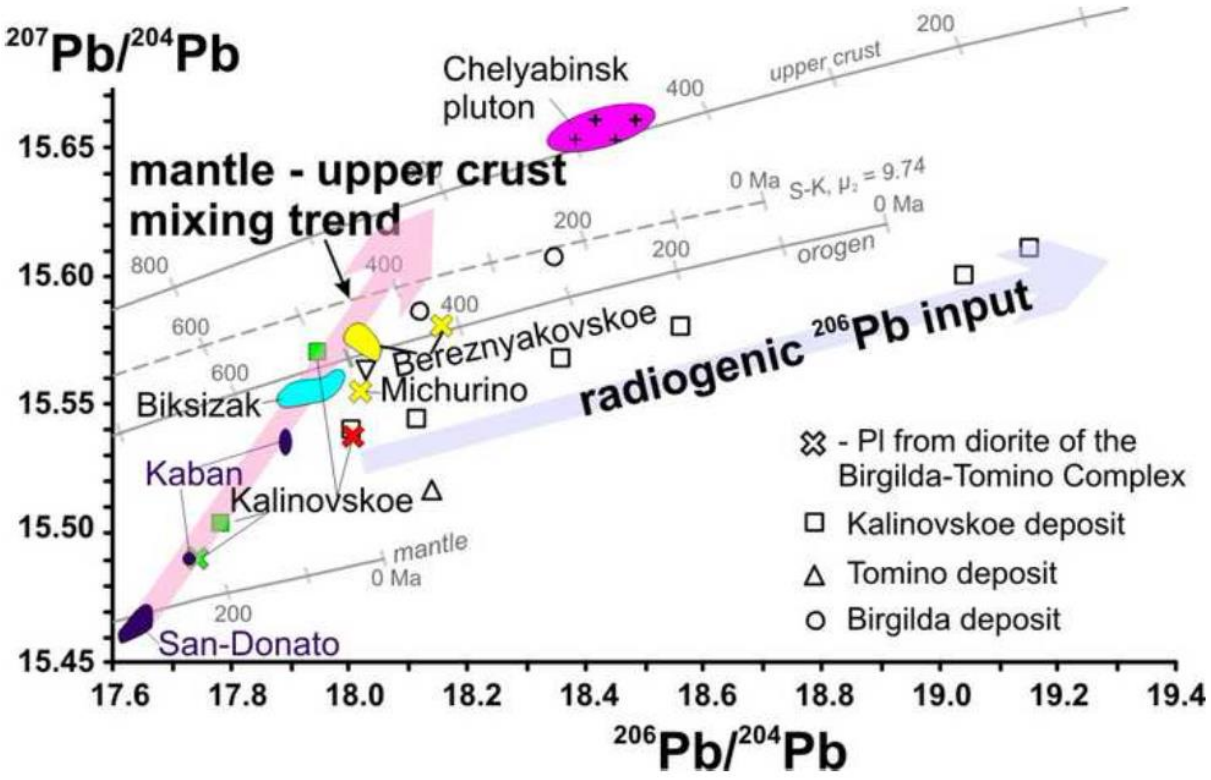

Highlights

- Distinctive Pb isotope values for porphyry-epithermal mineralization of the Birgilda-Tominoore cluster;
- Genetic relation between mineralization and intrusions of the Birgilda-Tomino igneous complex;
- Revealed variations in Pb isotopic composition are caused by a mixing of mantle and crustal Pb sources;
- Input of radiogenic ^{206}Pb took place in post-ore phaseas a result of multiple tectono-magmatic events.